A Novel EER Transmitter Using Two-Point Delta-Sigma Modulation Scheme for WLAN and 3G Applications

Kang-Chun Peng, Je-Kuan Jau, and Tzyy-Sheng Horng

Department of Electrical Engineering, National Sun Yat-Sen University, Kaoshiung 804, Taiwan

Abstract — **A novel transmitter architecture is proposed for wireless local area networks (WLAN) and 3rd generation (3G) mobile applications. The transmitter is based on the envelope elimination and restoration (EER) architecture applied with two-point delta-sigma modulator (TPDSM). It can integrate digital modulators and power amplifiers without mixers effectively. In addition, the power amplifier can deal with non-constant envelope modulations like QPSK highly efficiently.**

I. INTRODUCTION

High power conversion efficiency has been always an important task for designing a mobile RF transmitter to achieve a longer battery recharge cycle. Up to date a variety of transmitter architectures have been exploited to meet this goal. Fig. 1 shows a conventional direct-conversion transmitter architecture. It utilizes the quadrature modulation scheme to transfer the baseband signals to RF and requires two digital-to-analog converters (DAC), two well-matched mixers, a precise quadrature voltage-control oscillator (VCO) and a highly efficient power amplifier (PA). The requirement of PA's linearity depends on the modulation schemes. The non-constant envelope modulation like QPSK requires a highly linear PA. Unfortunately, for designing a PA it is usually a tradeoff between linearity and efficiency. Most highly linear PAs in mobile transceivers exhibit their best efficiencies only between 30% and 40% [1]. On the other hand, PA's linearity is not required for the constant envelope modulations like GFSK and GMSK. More efficient PA designs are applied under these modulation schemes.

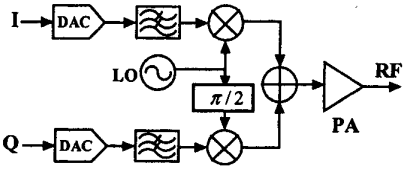

Fig. 1. A quadrature-modulation and direct-conversion transmitter architecture.

Fig. 2 shows the transmitter with the two-point delta-sigma modulator (TPDSM) proposed in [2] for GSM system, which can achieve high date rate for constant envelope modulations and has been used in Bluetooth system successfully [3]. This architecture is based on a familiar fractional-*N* synthesizer. The low-frequency components of the pulse-shaped baseband signal are frequency-modulated within the phase-locked loop (PLL) bandwidth through the delta-sigma modulator (DSM) while the high-frequency components are frequency-modulated outside the PLL bandwidth by applying the pulse-shaped baseband signal directly to the second tuning input of VCO. This scheme can resolve the problem of the modulation bandwidth limited to the PLL bandwidth. Another useful feature is that the TPDSM transmitter can exclude the use of mixers in GFSK modulation and up-conversion.

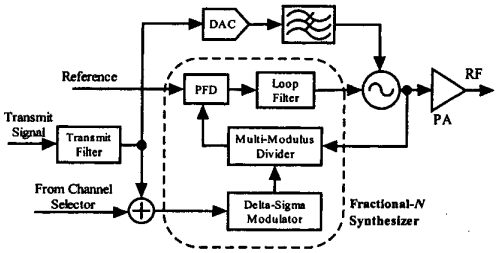

Fig. 2. A TPDSM transmitter architecture in Bluetooth system.

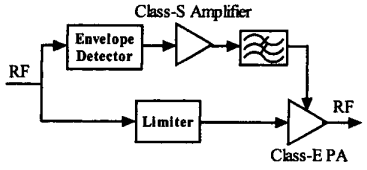

Fig. 3. A conventional EER transmitter architecture for high power conversion efficiency.

Fig. 3 shows an envelope elimination and restoration (EER) transmitter proposed in [4] for non-constant envelope modulations. This architecture utilizes a limiter and an envelope detector to extract the phase and envelope signals separately. Both signals are then amplified separately and recombined using a class-E PA that can be designed highly efficiently. In this paper, new

0-7803-7239-5/02/$10.00 © 2002 IEEE

transmitter architecture has been proposed by combining EER and TPDSM to possess the advantages of high data rate and conversion efficiency simultaneously for non-constant envelope modulations and will be generally good for WLAN and 3G applications.

II. Proposed Transmitter Architecture

Fig. 4 shows the proposed transmitter architecture. The rectangular-to-polar converter separates the envelope and phase information in digital domain. It is much more accurate than be done in analog domain with limiter and envelope detector in a conventional EER transmitter. After passing DAC and low-pass filter, the envelope signal was amplified by a low-frequency but high-efficiency class-S amplifier. In order to filter out the harmonics produced by the class-S amplifier, another analog low pass filter is placed behind.

In the other path, a TPDSM is utilized to transfer the baseband phase data to a constant-envelope phase modulation signal. Note that the TPDSM belongs to a frequency-modulation modulator. So the pre-processing digital differentiation of phase data with respect to time becomes required. In the output stage, a highly efficient class-E PA amplifies such a constant-envelope phase-modulation signal and multiplies the envelope signal from the other path that is applied as the supply voltage of class-E PA where the output voltage varies linearly with the supply voltage in principle.

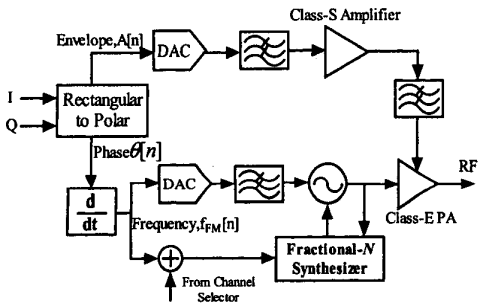

Fig. 4. Proposed transmitter architecture based on combination of EER and TPDSM.

III. Design Aspects

A. Resolution of DSM and DACs

One DSM and two DACs are utilized for modulating the baseband signal in the proposed architecture. Adequate choice of resolution for DSM and DACs is important because it determines the circuit complexity, power consumption and modulation accuracy. These resolution parameters can be generally expressed as

$$R_{DSM} = \log_2 \frac{f_s}{f_{res}} \quad \text{(Bits)}, \tag{1}$$

$$R_{DAC}^{f} = \log_2 \frac{V_{\max} K_{VCO}^{(2)}}{f_{res}} \quad \text{(Bits)}, \tag{2}$$

$$R_{DAC}^{a} = \log_2 \frac{V_{\max}}{E_{res}} \quad \text{(Bits)}. \tag{3}$$

It is noted that R_{DSM} represents the resolution bits for DSM used in the fractional-N synthesizer, while R_{DAC}^{f} and R_{DAC}^{a} represent the resolution bits for DACs used in the frequency-modulation path and envelope path, respectively. The circuit design parameters include $V_{\max}$ and $K_{VCO}^{(2)}$ that represent the maximum DAC dynamic range and tuning sensitivity (gain) in VCO's second input, respectively. From (1)-(3) the above parameters can further determine three dominant factors for modulation accuracy. They are f_s, f_{res}, and E_{res} that denote the sampling frequency, frequency-modulation resolution and envelope resolution, respectively.

B. Envelope Feedback

The delay mismatch between envelope and phase path in an EER transmitter should be considered carefully because it causes the inter-modulation distortion (IMD), which not only degrades the modulation but also causes the spectral regrowth. In [5] it has been shown that the resultant IMD for two-tone input can be approximated as

$$IMD \approx 2\pi B_{RF}{}^2 \tau_{EER}{}^2, \tag{4}$$

where B_{RF} is the bandwidth of RF signal and τ_{EER} is the corresponding path-delay difference. To reduce the IMD, an envelope feedback method proposed in [6] can be adopted, as shown in Fig. 5. This method utilizes an envelope detector together with an attenuator to extract the envelope signal from the amplified RF signal at the output of the class-E PA. After comparing the detected signal with the original envelope signal, the difference is applied to the input of class-S amplifier. This approach can make the transmitter insensitive to the path-delay difference that is mainly due to the use of low-pass filters in the envelope path. Under this condition, the class-E PA can be regarded as an amplitude modulator with almost constant amplitude-sensitivity to recombine the phase and envelope signals without too much distortion.

C. Pre-Distortion Filter

In the TPDSM scheme, the gain and delay mismatch between two modulation paths are also important factors

to cause distortion. In a similar fashion, the feedback loop for adjusting the gain and delay can be applied. However, it requires an additional RF phase demodulator that will complicate the transmitter circuit and lead to more power consumption. As also shown in Fig. 5, we proposed a digital pre-distortion filter to compensate such gain and delay mismatch in advance.

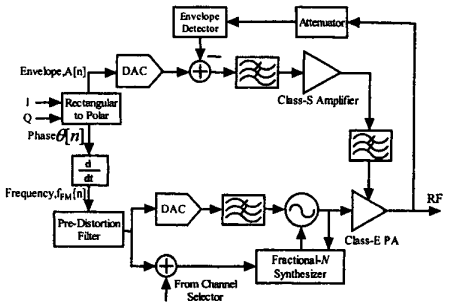

Fig. 5. Proposed transmitter architecture with envelope feedback and phase pre-distortion.

To optimize the pre-distortion filter design, a linear TPDSM model as shown in Fig. 6 has been analyzed. In the following formulation τ_1 and τ_2 denote the delays of two different modulation paths. The transfer function $G(S)$ is used to characterize the gain mismatch. The phase of transmitted signal is represented by ϕ_{sig}. The phase noises from VCO and reference source are represented by $\phi_{n,vco}$ and $\phi_{n,ref}$, respectively. The DSM generates the quantization noise represented by $\phi_{n,DSM}$. The phase of output signal can be finally expressed as

$$\phi_{out} = \phi_{sig} H_a(S) + \phi_{n,VCO} e^{-S\tau_2} H_e(S) + \left(\phi_{n,DSM} + \phi_{n,ref}\right) e^{-S\tau_1} H(S) \quad (5)$$

where

$$H(S) = \frac{NK_v K_d F(S)}{NS + K_v K_d F(S)}, \quad (6)$$

$$H_e(S) = \frac{NS}{NS + K_v K_d F(S)}, \quad (7)$$

$$H_a(S) = e^{-S\tau_1} H(S)/N + e^{-S\tau_2} G(S) H_e(S). \quad (8)$$

In (5) the transfer functions $H(S)$ and $H_e(S)$ depend on the PLL parameters which can be designed carefully to suppress the DSM quantization noise as well as the phase noises generated from VCO and the reference source. This leaves the transfer function $H_a(S)$ as the dominant factor to cause the distortion. Therefore, the pre-distortion filter can be used for compensation when its transfer function is specified as

$$C(S) = 1/H_a(S). \quad (9)$$

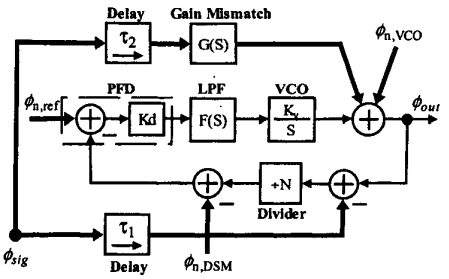

Fig. 6. A linear model for TPDSM.

IV. Simulation Results

The proposed transmitter was simulated for QPSK-modulated signals at 2 GHz. The data rate was set at 2 Mbps. The pulse-shaping filter adopted root-raised-cosine (RRC) filter with roll-off factor equal to 0.35. The maximum dynamic range of DAC was set at $V_{max} = 2.5$ volts. The tuning sensitivity of VCO's second input was set at $K_{VCO}^{(2)} = 55$ MHz/V. For the PLL parameters, the damping ratio was set at 0.7 and the natural frequency was set at 50 kHz. To simplify the simulation procedure, the DSM quantization noise was ignored.

At the beginning, the DSM sampling frequency was fixed at $f_s = 20$ MHz. By substituting the above-mentioned conditions into (1) and (2), we can find that R_{DSM} and R_{DAC}^f satisfy the relation: $R_{DSM} \approx R_{DAC}^f - 2$. In Fig. 7 the error vector magnitude (EVM) for the QPSK-modulated signal was simulated as a function of R_{DAC}^a when R_{DSM} and R_{DAC}^f were equal to 14 and 16 bits, respectively. It can be seen that $R_{DAC}^a \geq 5$ bits is good for maintaining EVM < 2%. Fig. 8 shows the simulated EVM by varying R_{DSM} and R_{DAC}^f together when R_{DAC}^a was exactly equal to 5 bits. It reveals that EVM will exceed 2%, 3% and 5% when R_{DAC}^f is less than 16 bits, 14 bits and 13 bits, respectively. Assuming that R_{DAC}^a and R_{DAC}^f were equal to 5 and 16 bits, respectively, we simulated the EVM by varying R_{DSM} under the condition of adjustable f_s. The results are demonstrated in Fig. 9. It can be seen that $R_{DSM} \geq 12$ bits is sufficient to reach EVM < 2%. Therefore, in the following simulations for output spectral regrowth and constellations, the resolution parameters R_{DSM}, R_{DAC}^f and R_{DAC}^a were set at 12 bits, 16 bits and 5 bits, respectively. The EVM under the conditions of perfect match in delay and gain among different modulation paths was predicted to be less than 2%.

Fig. 10 shows comparison of the simulated output spectral regrowth for generating the specified QPSK signal with and without envelope feedback. It was assumed that the envelope path has a larger delay by 50 ns

than the TPDSM path. However, for the two modulation paths inside TPDSM, perfect match in gain and delay was assumed. It can be seen from Fig. 10 that the envelope feedback can compensate the envelope delay effectively and therefore improve the sideband suppression by more than 10 dB.

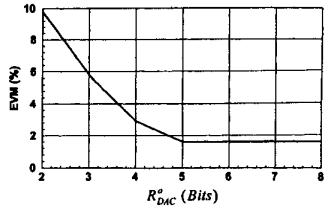

Fig. 7. Simulated EVM performance as a function of R^a_{DAC}. ($R_{DSM}=14$ bits and $R^f_{DAC}=16$ bits).

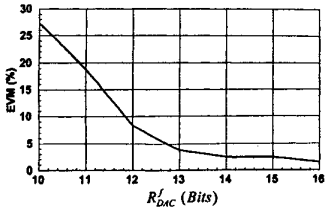

Fig. 8. Simulated EVM performance as a function of R^f_{DAC}. ($R^a_{DAC}=5$ bits and $R_{DSM}=R^f_{DAC}-2$ bits).

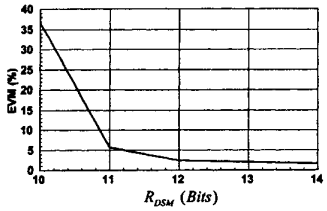

Fig. 9. Simulated EVM performance as a function of R_{DSM}. ($R^a_{DAC}=5$ bits and $R^f_{DAC}=16$ bits).

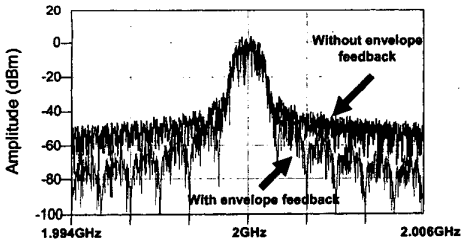

Fig. 10. Simulated output spectral regrowth for transmitting the specified QPSK signal.

Fig. 11 compares the simulated constellations with and without the pre-distortion filter when the path-delay difference ($\tau_2-\tau_1$) and gain mismatch factor $G(S)$ were assumed to be 50 ns and 1.05, respectively. It was also assumed that the delay in the envelope path was exactly equal to τ_1. In the absence of pre-distortion filter, the mismatch was not compensated at all, which resulted in significant magnitude and phase errors in the constellation. The corresponding EVM is about 13.81%. When the pre-distortion was present, the mismatch was improved obviously and the corresponding EVM was reduced to 1.44%.

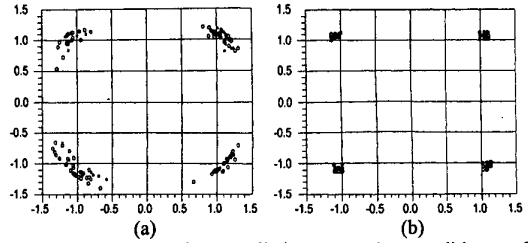

Fig. 11. Simulated constellations on the conditions of $\tau_2-\tau_1=50$ ns and $G(S)=1.05$ (a) without pre-distortion filter and (b) with pre-distortion filter.

V. Conclusion

A new and highly linear transmitter architecture for non-constant envelope modulations has been presented. It combines the EER and TPDSM schemes skillfully to obtain the major advantages in both schemes including extremely high date rate and conversion efficiency. Various design aspects for this transmitter have been addressed. An example for generating QPSK signal has been simulated to illustrate the potential technical barriers and their improvements.

Acknowledgment

This research was supported by the National Science Council, Taiwan R.O.C., under grant NSC90-2213-E-110-021. It was also supported in part by Ericsson Taiwan Ltd., under grant 90A2070.

References

[1] B. Razavi, *RF Microelectronics*, Prentice Hall, Inc., 1998.

[2] R.A. Meyers and P.H. Waters, "Synthesizer review for PAN-European digital cellular radio," in proc. *IEE Colloquium on VLSI Implementations for 2nd Generation Digital Cordless and Mobile Telecommunication Systems*, pp. 8/1-8/8, 1990.

[3] C. Durdodt, et. al.," The first very low-IF RX, 2-point modulation TX CMOS system on chip Bluetooth solution," in proc. *IEEE RFIC Symposium*, pp.99-102, 2001

[4] L.R. Kahn, "Single sideband transmission by envelope elimination and restoration," *Proc. IRE*, vol. 40, no.7, pp.803-806, July 1952.

[5] F.H. Raab, "Intermodulation distortion in Kahn-Technique transmitters," *IEEE Trans. Microwave Theory Tech.*, vol. 44, no. 12, pp. 2273 -2278, Dec. 1996.

[6] W.B. Bruene, "Distortion reducing means for single-side band transmitters," *Proc. IRE*, vol.44, no.12, pp. 1760-1765, Dec. 1956.